

Comparative Analysis of Early Dynamic Trends in Novel Coronavirus Outbreak: A Modeling Framework

Huazhen Lin^a, Wei Liu^a, Hong Gao^a, Jinyu Nie^a, Qiao Fan^b

^a*Center of Statistical Research and School of Statistics, Southwestern University of Finance and Economics, Chengdu, China*

^b*Centre for Quantitative Medicine, Program in Health Services & Systems Research, Duke-NUS Medical School, Singapore*

Abstract

Background The 2019 coronavirus disease (COVID-19) represents a significant public health threat globally. Here we describe efforts to compare epidemic growth, size and peaking time for countries in Asia, Europe, North America, South America and Australia in the early epidemic phase.

Methods Using the time series of cases reported from January 20, 2020 to February 13, 2020 and transportation data from December 1, 2019 to January 23, 2020 we have built a novel time-varying growth model to predict the epidemic trend in China. We extended our method, using cases reported from January 26, 2020 - or the date of the earliest case reported, to April 9, 2020 to predict future epidemic trend and size in 41 countries. We estimated the impact of control measures on the epidemic trend.

Results Our time-varying growth model yielded high concordance in the predicted epidemic size and trend with the observed figures in China. Among the other 41 countries, the peak time has been observed in 28 countries before or around April 9, 2020; the peak date and epidemic size were highly consistent with our estimates. We predicted the remaining countries would peak in April or May 2020, except India in July and Pakistan in August. The epidemic trajectory would reach the plateau in May or June for the majority of countries in the current wave. Countries that could emerge to be new epidemic centers are India, Pakistan, Brazil, Mexico, and Russia with a prediction of 10^5 cases for these countries. The effective reproduction

Email addresses: linhz@swufe.edu.cn (Huazhen Lin), qiao.fan@duke-nus.edu.sg (Qiao Fan)

Preprint submitted to Journal

April 19, 2020

number R_t displayed a downward trend with time across countries, revealing the impact of the intervention remeasures i.e. social distancing. R_t remained the highest in the UK (median 2.62) and the US (median 2.19) in the fourth week after the epidemic onset.

Conclusions New epidemic centers are expected to continue to emerge across the whole world. Greater challenges such as those in the healthcare system would be faced by developing countries in hotspots. A domestic approach to curb the pandemic must align with joint international efforts to effectively control the spread of COVID-19. Our model promotes a reliable transmissibility characterization and epidemic forecasting using the incidence of cases in the early epidemic phase.

Keywords: Coronavirus, COVID-19, SARS-CoV-2, transmissibility, outbreaks, reproduction number R , generalized growth modeling

1. Introduction

In early December 2019, a novel severe acute respiratory syndrome coronavirus, SARS-COV-2, emerged into the human population in Wuhan, China¹⁻⁷. The first coronavirus disease 2019 (COVID-19) case outside China was reported on January 13, 2020 in Thailand. In just several weeks, the local transmission started rapidly in a broad array of countries in Asia, Europe, North America, South America and Australia, with the emergence of new epicenters of spread, such as the US, Italy, Spain, and France (<https://www.who.int>). The rapid spreading of SARS-COV-2 has led to a major global public health threat. The World Health Organization (WHO) declared the spread of COVID-19 a pandemic on March 11, 2020.

Early epidemic forecasts consisting of the likely trajectory of an unfolding outbreak can help guide the type and intensity of interventions⁸⁻¹⁰. The vast majority of these approaches considered early exponential growth dynamics, an assumption that could lead to substantial overestimation of epidemic size and peak timing. To enhance the ability to forecast epidemics, it is crucial to characterize the shape of epidemic growth and accurately assess early trends of sub-exponential growth phenomenon¹¹⁻¹³. Currently, the global case count continues to rise, but there is a limited understanding of the extent of the outbreak and epidemic growth profile, particularly for the new emerging epicenters.

22 In this study, we attempt to assess and compare the extent of the out-
23 break across countries, draw preliminary conclusions about the impact of
24 control measures, and characterize real-time effective reproduction number
25 R_t . Our model, without making explicit assumptions about the epidemic
26 growth profile, is a generalizable framework to estimate the early dynamic
27 trends of COVID-19 from the incidences of cases. We estimated the epidemic
28 trend and size in China using the cases reported from January 20, 2020 to
29 February 13, 2020, and in other 41 countries using data from January 26,
30 2020, - or the date of the earliest case reported, to April 9, 2020.

31 **2. Methods**

32 *2.1. Sources of Data*

33 We obtained the number of COVID-19 confirmed cases of time series
34 data between January 20, 2020 to February 13, 2020 in China from the
35 official websites of the National Health Commission of China and Provincial
36 Health Committees (<http://www.nhc.gov.cn>). The data of cases for each
37 of the 29 provinces (25 provinces plus 4 municipalities including Beijing,
38 Shanghai, Chongqing and Tianjin) at 23 time points were included, as well
39 as for Wuhan and major cities in Hubei. The start date of January 20 was
40 chosen because the official diagnostic protocol released by WHO on January
41 17 allows the new COVID-19 cases to be diagnosed accurately and rapidly.
42 All cases were laboratory-confirmed with the detection of viral nucleic acid
43 following the case definition by the National Health Commission of China.

44 Wuhan is connected to other cities in China via high-speed railway, high-
45 way, and airplane flights. Population mobility statistics to estimate the ex-
46 posed sizes in cities outside Wuhan were based on transport-related databases
47 below: 1) Railway and airline travel data: the daily numbers of outbound
48 high-speed trains from Wuhan with corresponding travelling hours were ob-
49 tained from the high-speed rail network (<http://shike.gaotie.cn>) from Decem-
50 ber 1, 2019 to January 23, 2020, and similarly daily numbers of outbound
51 flight and hours for air transport were obtained from the Citytrip network
52 (<https://www.ctrip.com>) from December 1, 2019 to January 23, 2020. We
53 calculated daily travelling hours which equal to the product of the outbound
54 trip counts and the travelling hours for rail and air transport respectively
55 from Wuhan to each major city. For a given province, we summarized the
56 total number of travelling hours across all cities in that province. 2) Highway
57 mileage data: we collected highway mileage data from bus station networks at

58 <https://www.qichezhan.cn>. It contains the highway mileage from Wuhan to
59 16 cities in the Hubei Province. 3) Migration data: we obtained population
60 migration data from the Baidu Migration Map (<http://qianxi.baidu.com>)
61 which includes both the percentages and volumes of migration from Wuhan
62 to other cities and provinces from January 1 to 28, 2020. Total travelling
63 hours for rail and air flight, and migration scales are plotted by the province in
64 Supplementary Figure 1. Accumulated time on trains, on airplanes, highway
65 mileage and population migration scales were used to model the underlying
66 epidemic sizes in the provinces or cities outside Wuhan at the time 0 of this
67 study which is on January 20, 2020.

68 From Supplementary Figure 1, we observed that Guangdong has the
69 largest traveling hours through railway and airplane outbound from Wuhan
70 among the provinces. Also, the largest population has immigrated from
71 Wuhan to Henan. In Hubei province, Cities of Huanggang and Xiaogan are
72 the closest to Wuhan in terms of mileage and the scale of migration. These
73 simple observations are consistent with our result that Guangdong, Henan,
74 Huanggang and Xiaogan have the largest number of estimated primary in-
75 fected cases imported from Wuhan on January 20, 2020.

76 We obtained the number of COVID-19 confirmed cases in 41 countries
77 using data from January 23, 2020, or the date of the earliest case reported,
78 to April 9, 2020 from the official websites of WHO at <https://www.who.int>.
79 We included 41 countries with at least confirmed cases on April 9 2020 in five
80 continents: Asia, Europe, North America, South America, and Australia.

81 *2.2. Modelling the transmissibility of COVID-19*

82 We introduce the main notation here. All times are calendar times, mea-
83 sured in days since the start of the epidemic.

Y_{kt}	number of accumulated diagnosed case till day t ,
TR_k	daily traveling hours on trains from Wuhan,
FL_k	daily traveling hours on airplane from Wuhan,
RM_k	highway mileage from Wuhan,
MI_k	volumes of migration from Wuhan from January 1 to 28, 2020,
α_k	number of underlying primary infected cases,
W_{kt}	underline number of infected individuals who are infectious,
m	duration of infectious period (day),

84 where the subscript k represents country, province or city k , the subscript t
85 represents day t . TR_k and FL_k are constructed based on the two reasons.
86 One is that the longer people stay on the train or plane, the more likely
87 he(she) is to get infected. Another is that the infection happens in local
88 area, hence the number of trains or planes has more information than the
89 population taking trains or planes. In addition, in Hubei province, most
90 people left Wuhan by cars, we use RM_k as one of measurement for the spatial
91 distance between city k and Wuhan.

92 2.2.1. Modeling for 28 provinces

93 First, we build an index α_k to represent the baseline infected cases in
94 province k on 20 January, 2020. Particularly, we will use TR_k , FL_k and MI_k
95 to measure the relationship between province k and Wuhan. We suppose

$$\alpha_k = \beta_1 \times TR_k + \beta_2 \times FL_k + \beta_3 \times MI_k, \text{ for province } k, \quad (1)$$

96 where $\beta = (\beta_1, \beta_2, \beta_3)'$ are estimated by the observed Y_{kt} in provinces $k =$
97 $1, \dots, K$ and $t = 1, \dots, T$.

98 So far, we are not sure the key epidemiological parameters that affected
99 spread and persistence. We hence make assumptions as least as possible. It is
100 obvious that the average cases in province k diagnosed at day t is proportional
101 to the scale of infectious cases on day $t-1$, $W_{k,t-1}$. We then assume a Poisson
102 distribution for the new cases diagnosed in province k at day t with mean
103 $\gamma_{kt}W_{k,t-1}$, that is

$$dY_{kt} = Y_{kt} - Y_{k,t-1} \sim \text{Poisson}(\gamma_{kt}W_{k,t-1}), \quad (2)$$

104 where ' \sim ' means 'distributed as'.

105 Under the unified leadership of the central government, we suppose the
106 trend of γ_{kt} over day t is the same for 28 provinces, that is, $\eta_{kt} = \eta_t$ is
107 independent of k so that

$$\gamma_{kt} = \eta_t \times \gamma_{k,t-1}. \quad (3)$$

108 To avoid strong assumptions about the evolution of the epidemic, we allow
109 η_t to be arbitrary function of t . We determine the functional form of η_t by
110 pointwise estimating η_t and checking the resulting pattern over t . Denote
111 the resulting functional form for η_t by $\eta_t = \eta_t(a)$.

112 The new cases diagnosed at day t may be not reported fully. That is,

113 $E(dY_{kt}) = pdW_{kt}$ and $p < 1$. The estimation for p need more information
 114 except that we have. Fortunately, simple mathematical derivation shows
 115 that the value of p may influence the prediction of the absolute epidemic size
 116 but will not affect the trend of the epidemic, for example, the reproduction
 117 number, the duration and the peak time of the epidemic and relative epidemic
 118 size, in which we are interested. Hence, we suppose $p = 1$ in the paper. Since

$$W_{kt} = W_{k,t-1} + dW_{kt}, \quad dW_{kt} = E(dY_{kt}) = \gamma_{kt}W_{k,t-1}. \quad (4)$$

119 With the chain calculation, we have $dW_{kt} = \gamma_{kt} \prod_{j=0}^{t-1} (\gamma_{kj} + 1)W_{k0}$ and $W_{kt} =$
 120 $\prod_{j=0}^{t-1} (\gamma_{kj} + 1)W_{k0}$, where $W_{k0} = \alpha_k$ and $\gamma_{k0} = 0$. In practice, the infected
 121 patients will be isolated and removed from the infectious source. With the
 122 notation m of duration of infectious period, we hence have

$$W_{kt} = \prod_{j=0}^{t-1} (\gamma_{kj} + 1)\alpha_k - I(t > m) \prod_{j=0}^{t-(m+1)} (\gamma_{kj} + 1)\alpha_k. \quad (5)$$

123 Denote $\gamma_1 = (\gamma_{11}, \dots, \gamma_{K1})'$ and all of the parameters by $\delta = (\gamma'_1, a', \beta')'$.
 124 Taken (1), (2), (3) and (5) together, the loglikelihood function was

$$\begin{aligned} L(\delta) &= \sum_{k=1}^K \sum_{t=1}^T \{dY_{kt} \log(\lambda_{kt}) - \lambda_{kt}\} + C \\ &= \sum_{k=1}^K \sum_{t=1}^T (dY_{kt} \log[\gamma_{kt} X_k^T \beta \{\prod_{i=1}^{t-1} (1 + \gamma_{ki}) - I(t > m) \prod_{i=1}^{t-m} (1 + \gamma_{ki})\}]) \\ &\quad - \gamma_{kt} X_k^T \beta \{\prod_{i=1}^{t-1} (1 + \gamma_{ki}) - I(t > m) \prod_{i=1}^{t-m} (1 + \gamma_{ki})\}) + C, \end{aligned} \quad (6)$$

125 where C is a constant independent of δ , m is determined by minimizing
 126 the prediction error. The confidence intervals were obtained based on 200
 127 bootstrap resampling^{14, 15}.

128 2.2.2. Modeling for Hubei, Wuhan and the other countries

129 The modeling and the loglikelihood function for Hubei are similar with
 130 those for 28 provinces except that FL_k is replaced by RM_k and provinces are
 131 replaced by cities, because there are not flights between the cities in Hubei
 132 and Wuhan, and the most people leave Wuhan by cars or buses. Specifically,

$$\alpha_k = \beta_1 \times TR_k + \beta_2 \times RM_k + \beta_3 \times MI_k, \quad \text{for city } k \text{ in Hubei.} \quad (7)$$

133 The modeling and the likelihood function for Wuhan and countries, in-
134 cluding Singapore, South Korea, Japan, Italy, German, Spain, France and
135 Iran, are similar with those for 28 provinces except that α_k is directly esti-
136 mated by the diagnosed cases in Wuhan and other 41 countries respectively.

137 2.2.3. The calculation of the time-dependent reproduction number R_t

138 The equation $dW_{kt} = \gamma_{kt}W_{k,t-1}$ implies that, when $W_{k,t-1} = 1$, we have
139 $\gamma_{kt} = dW_{kt}$. Hence γ_{kt} is the average number of new infections created by an
140 infectious individual in one day, then $\phi_t = \sum_{k=1}^K \gamma_{kt}/K$ is the corresponding
141 average number across provinces or cities. Since one infectious individual
142 can make infection for m days, an infectious individual then can lead to
143 $R_t = m\phi_t$ new infections, which indeed is the time-dependent reproduction
144 number^{16, 17}.

145 2.2.4. Predication of potential peak time and turning point in COVID-19 146 outbreak

147 With the estimated parameters by maximizing the loglikelihood (6), we
148 can estimate and predict the average new cases $dW_{kt} = \gamma_{kt} \prod_{j=0}^{t-1} (\gamma_{kj} + 1)\alpha_k$,
149 then the cumulative cases $\tilde{W}_{kt} = \prod_{j=0}^t (\gamma_{kj} + 1)\alpha_k$. Based on the new cases
150 and cumulative cases, we can predict the peak time and the turning point in
151 the COVID-19 outbreak. In the paper, we defined the peak time to be the
152 day at which the incidence cases began to decline, and the turning point to
153 be the day when the number of the cumulative cases reached a plateau, which
154 satisfying $|\partial f(v)/\partial v| \leq c_0$, where $f(v) = \frac{\partial \tilde{W}_{kt}/\partial t|_{t=v}}{\partial \tilde{W}_{kt}/\partial t|_{t=v-1}}$ and c_0 is a prespecified
155 small number. We take $c_0 = 2e - 03$ through the analysis.

156 3. Results

157 3.1. Fitting a generalized growth model using a time-series data

158 We fit the time-varying generalized growth model using the early stage
159 outbreak series data for Wuhan, Hubei province, China, and other 41 coun-
160 tries with at least 2,000 confirmed cases on the date of April 9 2020. The
161 optimal fitted model for each country or region was chosen based on the
162 prediction error of the lowest values (Supplementary Figures 2 to 4). The
163 corresponding empirical distributions of the parameters are shown in Table
164 1. The parameter m , the estimated mean infectious duration, ranged from 4
165 to 13 days, with the highest value of 13 for the epidemic in Italy. The short

166 duration of 4 days was estimated for South Korea. The value of m reflects
167 the duration of infectious period, which in practice could be intervened by
168 control measures such as early diagnosis and isolation. Another parameter
169 $\eta(t)$ quantifies how rapidly the growth rate $\gamma(t)$ at time t changed; the func-
170 tional form of $\eta(t)$ was estimated by pointwise estimation using data till t for
171 each model respectively. The growth rates declined most rapidly in China
172 and Thailand (median η : 0.86 to 0.89), and most slowly in India, Mexico,
173 Singapore and Sweden (median η : 0.98 to 0.99).

174 *3.2. Predictive performance of model fitting*

175 Using the calibrated model based on m and the form of $\eta(t)$, we esti-
176 mated the real-time growth rates based on the number of confirmed cases at
177 $t = 1, \dots, T$ by maximizing the likelihood function displayed in the Method
178 section. The underlying growth process was lower than the constant expo-
179 nential growth rate as medium $\eta(t)$ was consistently estimated at less than
180 1 (Supplementary figure 3), similar to findings of sub-exponential growth dy-
181 namics for epidemics of influenza, Ebola etc with the deceleration growth
182 factor below 1^{18, 19}.

183 For China, we used case incidence data from January 20 to February 13
184 as the epidemic reporting period to fit the model for trajectory predictions.
185 The observed values fall within 95% CI of the prediction band in general,
186 suggesting a good model fitting (Figure 1 and Supplementary Figures 8-9).
187 We predicted that the epidemics would fade out around February 19 to 24
188 across the 28 provinces, about 4 weeks after the intervention starting from
189 January 20; this is in concordance with the actual timing in which no more
190 new cases were observed at the end of February (<http://www.nhc.gov.cn>).
191 For 28 provinces in China, the estimated size was at 8553 to 9460 and 11,000
192 to 12,600 for Hubei province; both 95% CI estimates cover the observed
193 figures (Table 2). For Wuhan, due to the changes in the diagnosis criteria,
194 the predicted number of cases was not comparable after February 13. We
195 estimated the epidemic would fade out around the end of February, which is
196 close to the final date in which no more new cases were observed in Wuhan.

197 Within each province, the observed final epidemic size was within the 95%
198 CIs of prediction except 5 provinces, yet the prediction was still within 10%
199 +/- flanking the upper or lower bound (Supplementary Table 1). Given the
200 intervention measures are similar across provinces in China besides Hubei,
201 it is not surprising that we observed the trend that the provinces with a
202 higher estimated risk of imported cases α from Wuhan had an increased

203 epidemic size. However, there were some exceptions. For example, Bei-
204 jing ($\alpha = 28$; 95%CI : 7 – 49) and Shanghai ($\alpha = 16$; 4 – 28) were in the
205 high-risk group but the final infection numbers were 286 and 261. On the
206 contrary, Heilongjiang was in the low-risk group ($\alpha = 4 : 1 – 6$) whereas the
207 final infections were at 252. This implies the stronger intervention locally or
208 compliance in densely populated municipalities (Beijing or Shanghai), than
209 that in Heilongjiang, the north-east region far away from Wuhan. Over-
210 all our time-varying growth model provides a good fitting using time-series
211 confirmed cases for the epidemic of COVID-19 in China.

212 *3.3. Projection of the epidemic and final size in 41 countries*

213 We projected the future growth trajectory underlying the outbreak using
214 the daily confirmed case data from January 23, 2020 - or the date of the
215 earliest case reported - to April 9, 2020 in 42 countries across Asia, Europe,
216 North America, South America and Australia. Our prediction is based on the
217 estimated parameters assuming the sustainability of intervention measures.
218 The time-varying growth model fitting to the time-series data performed
219 well as shown by the observed cases generally falling in the 95% CI of the
220 prediction bound in each plot (Figure 1 and Supplementary Figures 8-12),
221 except for South Korea in the very early phase. The predicted cases were
222 higher than the observed number of infections from February 8 to 25, likely
223 due to a proportion of infections being greatly understated - the hiding cases
224 from the religious group.

225 We predicted the epidemic size and duration of the outbreak with the
226 assumption of current model fitting parameters (Table 2). In Asia, the epi-
227 demic will continue until May in Philippine, Malaysia and Iran, and July in
228 Indonesia. Strikingly, the epidemic would have the longest outbreak spread
229 until February or March 2021 in Indian and Pakistan, with the final infec-
230 tions at more than a million. For Japan and Singapore, we were not able
231 to do predictions on the epidemic sizes and duration because the estimated
232 time-varying growth rates kept on increasing at the end of the study period
233 – which is concordant to the big daily jump in cases observed in these two
234 countries recently; thus incidence case data in a longer period are required for
235 valid predictions using our model. In Europe, the epidemic will not fade out
236 until May or June for the majority of countries. However the epidemic may
237 last until August (Russia and Sweden). In North America, the epidemic will
238 continue until May (Canada, Dominican Republic), June (US) and October
239 (Mexico), and the infection are estimated to be around 1 million in the US,

240 and 10^5 in Mexico. In South America, the epidemic will continue until May
241 (Chile) and June (Brazil, Colombia and Panama). Among them, Brazil has
242 the largest estimated infections with more than 10^5 .

243 *3.4. Estimation of peak time*

244 We estimated the peak time, the day at which the incidence cases began
245 to decline based on the estimated daily cases dW_{kt} (see [Methods](#)). Among 41
246 countries, the peak time has been observed in 28 countries before or around
247 April 9, 2020 (Table 3 & Supplementary Figures 13-15). The estimations
248 in the above countries are concordant to the observed period during which
249 incidence cases declined. For other countries, under the current parameters
250 with continuity of intervention measures, we estimated the epidemic would
251 peak in April or May 2020 for the majority of countries, except for India
252 (July) and Pakistan (August). The predicted numbers of accumulated cases
253 at the peak point were also consistent with the observed figures. Based on
254 the predicted number of infections, we estimated the maximum number of
255 ventilators for the peak requirement. For example, at least 500,000 venti-
256 lators need to be prepared for the epidemic peak in India, $\sim 100,000$ for
257 Pakistan. Considering the death or recovery rate, the number is regarded as
258 the upper bound in practice.

259 *3.5. Impact of the reduction of the infectious period*

260 Shortening the time from the infection onset (symptomatic or asympto-
261 matic) to isolation, termed as ‘infectious period’ in this paper, is vital as
262 it will reduce transmission. The control strategies could rely on social dis-
263 tancing, earlier isolation of cases and population-based testing to identify
264 the presymptomatic or asymptomatic cases. Here we evaluated the impact
265 of shortening the infectious period on the epidemics, showings the epidemic
266 curve for each country, assumed to be 1 or 2 days shorter in the duration
267 of infectivity infectious period (Supplementary Figures 13-15). A reduction
268 of the infectious period by 1 or 2 days would have a negligible effect on the
269 peak time, as the estimation was essentially the same. The reduction of the
270 infectious period by 1 or 2 days would lead to a significantly flatted epidemic
271 curve across all the countries. For example, the 2-days decrease in the in-
272 fectious period would result in a significant reduction of the final epidemic
273 size in India (31.1%), Pakistan (39.3%), Russia (22.6%), Brazil (26.8%), and
274 Mexico(18.0%).

275 *3.6. Estimation of real-time effective reproduction number R_t*

276 We quantified the real-time reproduction number R_t (see [Method sec-](#)
277 [tion](#))^{17, 20, 21}, based on the estimation parameters of growth rates γ and the
278 infectious period m . The R_t exhibited a declining trend with time and vari-
279 ability in the estimates across countries (Table 4). The uncertainty of R_t
280 was largest in the first week and gradually became smaller with time (Table
281 4). In the first week, 28 countries displayed R_t below 5 while 14 exhibited
282 large R_t above 5. Italy and Spain displayed the highest R_t at 12.36, and 9.26
283 respectively. R_t estimations become closer ranging from 0.95 (Singapore)
284 to 5.54 (Spain) in the second week. During the first month of the epidemic
285 period, all countries displayed a declined trend towards 1 in the epidemic pe-
286 riod with varying deceleration rates, revealing the impacts of the intervention
287 strategies. In the fourth week, 14 countries exhibited R_t below 1, the highest
288 in UK (2.62) and the US (2.19). For Singapore and Japan, although both
289 displayed the declining trend in the first month, there is an inclining trend
290 starting from April, implying the intervention could not be effective in the
291 late stage (Supplementary Figure 16). R_t displayed the fastest deceleration
292 in China with the most pronounced changes during the third to fourth weeks;
293 this may reveal the significant impact of intervention measures implemented
294 since January 20, 2020 in the first week.

Table 1: Summary of fitting parameters for the selected model in 10 countries in 2020.

	Epidemic study period	m	Medium η_t (95%)	form of η_t
Asia				
China	01/20– 02/13	6	0.89(0.87, 0.91)	$a_0 + a_1(t - t_1)_- + a_2(t - t_2)_-$
Hubei Province, China	01/20– 02/13	9	0.86(0.84, 0.88)	$a_0 + a_1(t - t_1)_- + a_2(t - t_2)_-$
Wuhan, China	01/20– 02/13	6	0.88(0.86, 0.90)	$a_0 + a_1(t - t_1)_- + a_2(t - t_2)_-$
India	03/04–04/09	9	0.99(0.98, 1.00)	$a_0 + a_1(t - t_1)_-$
Indonesia	03/08–04/09	10	0.97(0.96, 0.98)	$a_0 + a_1(t - t_1)_-$
Iran	03/19–04/09	8	0.96(0.96, 0.98)	$a_0 + a_1(t - t_1)_-$
Japan	02/14–04/09	8	0.97(0.96, 0.98)	$a_0 + a_1(t - t_1)_-$
South Korea	01/24– 04/09	4	0.93(0.92, 0.94)	$a_0 + a_1(t - t_1)I(t_1 \leq t \leq t_2) + a_1(t_2 - t_1)I(t > t_2)$
Malaysia	02/27–04/09	11	0.94(0.93, 0.95)	$a_0 + a_1(t - t_1)_- + a_2(t - t_2)_-$
Pakistan	03/09–04/09	6	0.92(0.89, 0.95)	$a_0 + a_1(t - t_1)_- + a_2(t - t_2)_-$
Singapore	01/23–04/09	5	0.99(0.98, 1.00)	$a_0 + a_1(t - t_1)_-$
Thailand	03/09–04/09	10	0.89(0.88, 0.90)	a_0
Israel	03/03–04/09	7	0.92(0.90, 0.94)	a_0
Saudi Arabia	03/08–04/09	10	0.96(0.94, 0.98)	a_0
Turkey	03/15–04/09	6	0.90(0.89, 0.91)	$a_0 + a_1(t - t_1)_-$
North America				
US	02/24–04/09	6	0.94(0.93, 0.95)	$a_0 + a_1(t - t_1)_-$
Canada	02/27–04/09	8	0.94(0.93, 0.95)	$a_0 + a_1(t - t_1)_- + a_2(t - t_2)_-$
Dominican Republic	03/19–04/09	11	0.92(0.88, 0.96)	$a_0 + a_1(t - t_1)_-$
Mexico	03/13–04/09	11	0.98(0.96, 1.00)	a_0
South America				
Brazil	03/09–04/09	8	0.97(0.95, 0.99)	$a_0 + a_1(t - t_1)_- + a_2(t - t_2)_-$
Chile	03/10–04/09	7	0.94(0.93, 0.95)	$a_0 + a_1(t - t_1)_- + a_2(t - t_2)_-$
Colombia	03/10–04/09	8	0.96(0.94, 0.98)	$a_0 + a_1(t - t_1)_- + a_2(t - t_2)_-$
Panama	03/10–04/09	10	0.95(0.93, 0.97)	$a_0 + a_1(t - t_1)_-$
Europe				
Austria	02/29–04/09	10	0.90(0.88, 0.92)	$a_0 + a_1(t - t_1)_- + a_2(t - t_2)_-$
Belgium	03/01–04/09	10	0.94(0.93, 0.95)	$a_0 + a_1(t - t_1)_- + a_2(t - t_2)_-$
Czechia	03/03–04/09	7	0.94(0.93, 0.95)	$a_0 + a_1(t - t_1)_-$
Finland	03/05–04/09	8	0.97(0.96, 0.98)	$a_0 + a_1(t - t_1)_- + a_2(t - t_2)_-$
France	02/27–04/09	6	0.96(0.94, 0.98)	$a_0 + a_1(t - t_1)_-$
Germany	02/26–04/09	7	0.94(0.93, 0.95)	a_0
Ireland	03/08–04/09	7	0.94(0.93, 0.95)	$a_0 + a_1(t - t_1)_-$
Italy	02/21–04/09	13	0.93(0.92, 0.94)	$a_0 + a_1(t - t_1)_-$
Luxembourg	03/10–04/09	6	0.90(0.89, 0.91)	$a_0 + a_1(t - t_1)_-$
Netherlands	02/28–04/09	7	0.94(0.93, 0.95)	$a_0 + a_1(t - t_1)_-$
Norway	02/28–04/09	6	0.93(0.92, 0.94)	$a_0 + a_1(t - t_1)_- + a_2(t - t_2)_-$
Philippines	03/05–04/09	6	0.93(0.91, 0.95)	a_0
Poland	03/07–04/09	9	0.95(0.94, 0.96)	a_0
Portugal	03/03–04/09	11	0.92(0.91, 0.93)	$a_0 + a_1(t - t_1)_- + a_2(t - t_2)_-$
Romania	03/04–04/09	7	0.95(0.94, 0.96)	a_0
Russia	03/11–04/09	9	0.97(0.96, 0.98)	a_0
Spain	02/25–04/09	9	0.93(0.92, 0.94)	a_0
Sweden	02/29–04/09	12	0.98(0.97, 0.99)	a_0
Switzerland	02/29–04/09	10	0.93(0.92, 0.94)	a_0
United Kingdom	02/26–04/09	11	0.95(0.94, 0.96)	a_0
Australia				
Australia	02/29–04/09	8	0.92(0.91, 0.93)	$a_0 + a_1(t - t_1)_- + a_2(t - t_2)_-$

Table 2: Estimation of median growth rate, final epidemic size and ending date for each country

Region	γ_t (95% CI)	Ending date		Final epidemic size		
		Prediction	Observation	Prediction	Observation	
Asia						
China	0.107(0.097, 0.117)	2020/02/22	2020/02/22	8553 ~ 9460	8666	
Hubei Province, China	0.177(0.151, 0.203)	2020/02/25	2020/02/25	1.10e4 ~ 1.26e4	1.14e4	
Wuhan, China	0.197(0.039, 0.355)	2020/02/29	2020/03/02	-	-	
India	0.215(0.175, 0.254)	2021/02/03	-	> 1e6	-	
Indonesia	0.162(0.138, 0.185)	2020/07/22	-	18648 ~ 83899	-	
Iran	0.141(0.130, 0.151)	2020/05/25	-	1.01e5 ~ 1.32e5	-	
Japan	0.099(0.088, 0.110)	-	-	-	-	
South Korea	0.150(0.129, 0.171)	2020/04/14	-	8469 ~ 12449	-	
Malaysia	0.174(0.147, 0.200)	2020/05/11	-	4994 ~ 6271	-	
Israel	0.323(0.261, 0.386)	2020/05/10	-	9636 ~ 17046	-	
Pakistan	0.211(0.180, 0.243)	2021/03/04	-	> 1e6	-	
Philippines	0.277(0.189, 0.364)	2020/05/31	-	6778 ~ 10201	-	
Saudi Arabia	0.216(0.188, 0.243)	2020/06/23	-	9302 ~ 21866	-	
Singapore	0.089(0.079, 0.098)	-	-	-	-	
Thailand	0.187(0.172, 0.202)	2020/04/27	-	2328 ~ 2956	-	
Turkey	0.314(0.297, 0.331)	2020/05/29	-	91290 ~ 123019	-	
North America						
US	0.368(0.336, 0.400)	2020/06/04	-	984100 ~ 1216034	-	
Canada	0.312(0.247, 0.378)	2020/05/12	-	43866 ~ 105344	-	
Dominican Republic	0.150(0.109, 0.191)	2020/05/30	-	7751 ~ 11364	-	
Mexico	0.167(0.144, 0.190)	2020/10/16	-	> 1e5	-	
South America						
Chile	0.227(0.190, 0.264)	2020/05/23	-	11536 ~ 15342	-	
Brazil	0.212(0.175, 0.249)	2020/06/04	-	> 1e5	-	
Colombia	0.187(0.160, 0.213)	2020/06/13	-	17692 ~ 105180	-	
Panama	0.199(0.171, 0.226)	2020/06/20	-	7250 ~ 15462	-	
Europe						
Austria	0.246(0.215, 0.277)	2020/04/26	-	12769 ~ 15887	-	
Belgium	0.241(0.210, 0.272)	2020/05/09	-	44728 ~ 53322	-	
Czechia	0.216(0.192, 0.239)	2020/05/13	-	6441 ~ 9609	-	
Finland	0.144(0.115, 0.172)	2020/06/09	-	9263 ~ 23582	-	
France	0.221(0.179, 0.263)	2020/06/15	-	> 3e5	-	
Germany	0.249(0.223, 0.275)	2020/05/21	-	1.43e5 ~ 1.88e5	-	
Ireland	0.211(0.181, 0.241)	2020/05/19	-	9414 ~ 15730	-	
Italy	0.180(0.169, 0.192)	2020/05/07	-	1.58e5 ~ 1.81e5	-	
Luxembourg	0.150(0.130, 0.170)	2020/04/29	-	2933 ~ 3907	-	
Netherlands	0.207(0.193, 0.220)	2020/06/07	-	31582 ~ 40301	-	
Norway	0.177(0.153, 0.202)	2020/05/07	-	5351 ~ 9636	-	
Poland	0.209(0.191, 0.228)	2020/06/22	-	13693 ~ 28531	-	
Portugal	0.290(0.250, 0.329)	2020/05/12	-	16759 ~ 22456	-	
Romania	0.241(0.198, 0.285)	2020/06/20	-	5822 ~ 22280	-	
Russia	0.268(0.235, 0.300)	2020/08/06	-	> 3e5	-	
Spain	0.274(0.238, 0.310)	2020/05/18	-	184932 ~ 219819	-	
Sweden	0.123(0.103, 0.143)	2020/08/31	-	> 8e4	-	
Switzerland	0.191(0.170, 0.212)	2020/05/14	-	25285 ~ 32773	-	
United Kingdom	0.283(0.242, 0.325)	2020/06/11	-	92514 ~ 312237	-	
Australia						
Australia	0.266(0.233, 0.298)	2020/04/16	-	4932 ~ 6969	-	

The ending date is the day when the number of the cumulative cases reach a plateau (see [Methods](#)). For Japan and Singapore, the predicted trend does not reach a plateau because of increasing growth rate at last time points (Supplementary Figure 3(h) & 4(h))

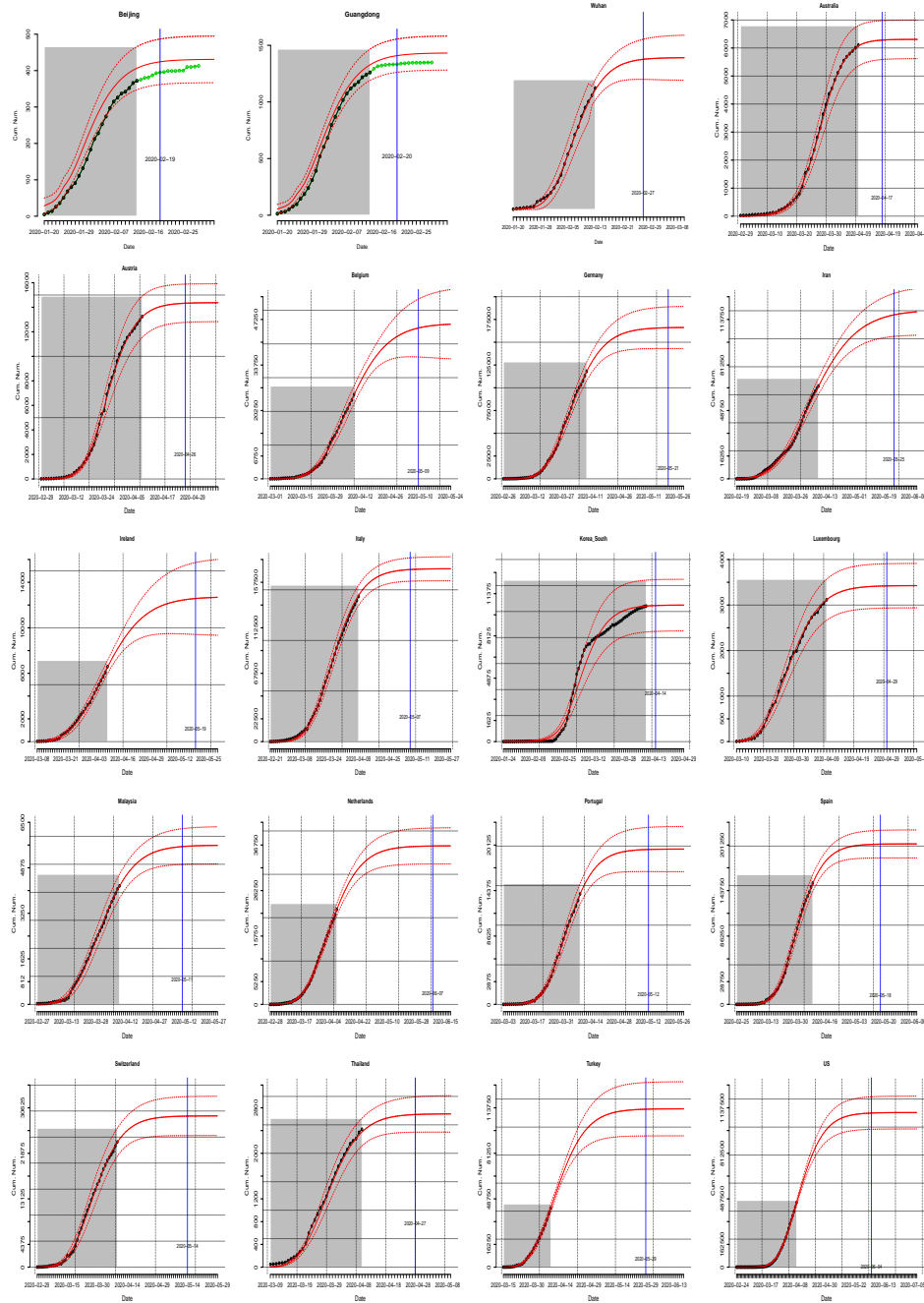


Figure 1: The estimated (red-solid) and observed (black-dotted) cumulative number of infectious over time t , as well as 95% CI (red-dashed) of the estimators. In addition, the green dots in the plot for Beijing and Guangdong in China refer to the number of reported cases which were not included for the model fitting.

Table 3: The predicted or observed peak date and the corresponding cumulated size among the different countries

	Peak date		# Maximum cases at the peak		# Ventilator needed for the peak
	Prediction	Observation	Prediction	Observation	
Asia					
India	2020/07/18	-	> 1e6	-	> 5e5
Indonesia	2020/04/24	-	7804	-	390 ~ 780
Iran	2020/04/03	2020/03/28-04/05	51615	47226	2581 ~ 5162
Israel	2020/04/01	2020/03/24-04/08	5929	5717	296 ~ 593
SKorea	2020/03/04	2020/02/25-03/10	4435	4693	222 ~ 444
Japan	-	-	-	-	-
Malaysia	2020/03/29	2020/03/24-04/02	2469	2382	123 ~ 247
Pakistan	2020/08/05	-	1.20e6	-	6.01e4 ~ 1.20e5
Philippines	2020/04/04	2020/04/03-04/06	2914	3254	146 ~ 291
Saudi Arabia	2020/05/13	-	26803	-	1340 ~ 2680
Singapore	-	-	-	-	-
Thailand	2020/03/28	2020/03/22-03/29	1222	987	61 ~ 122
Turkey	2020/04/14	2020/04/11-04/16	65276	63144	3264 ~ 6528
North America					
US	2020/04/09	2020/04/04-04/16	459761	489999	22988 ~ 45976
Canada	2020/04/08	2020/04/02-04/09	19208	15836	960 ~ 1921
Dominican Republic	2020/04/16	-	3512	-	176 ~ 351
Mexico	2020/05/23	-	60307	-	3015 ~ 6031
South America					
Chile	2020/04/07	2020/04/03-04/16	5071	6212	254 ~ 507
Brazil	2020/05/22	-	3.167927e+05	-	15839 ~ 31679
Colombia	2020/04/30	-	8173	-	409 ~ 817
Panama	2020/04/12	2020/04/09-04/12	3083	2872	154 ~ 308
Europe					
Austria	2020/03/26	2020/03/23-03/29	6641	6710	332 ~ 664
Belgium	2020/04/05	2020/04/02-04/07	19368	18875	968 ~ 1937
Czechia	2020/04/01	2020/03/28-04/05	3556	3586	178 ~ 356
Finland	2020/04/19	-	4242	-	212 ~ 424
France	2020/04/14	2020/04/10-04/16	1.60e5	1.21e5	8022 ~ 16043
Germany	2020/03/31	2020/03/24-04/08	72246	74873	3612 ~ 7225
Ireland	2020/04/06	2020/04/09-04/11	5421	7864	271 ~ 542
Italy	2020/03/25	2020/03/16-03/31	7.54e4	6.68e4	3771 ~ 7541
Luxembourg	2020/03/27	2020/03/21-03/31	1573	1434	79 ~ 157
Netherlands	2020/04/03	2020/04/02-04/10	15710	18862	786 ~ 1571
Norway	2020/03/23	2020/03/22-03/27	2659	3012	133 ~ 266
Poland	2020/04/12	2020/04/05-04/11	6796	5207	340 ~ 680
Portugal	2020/04/02	2020/03/31-04/10	8884	11196	444 ~ 888
Romania	2020/04/11	2020/04/09-04/16	5943	6424	297 ~ 594
Russia	2020/05/11	-	141110	-	7056 ~ 14111
Spain	2020/03/30	2020/03/25-04/01	87412	76795	4371 ~ 8741
Sweden	2020/05/09	-	37389	-	1869 ~ 3739
Switzerland	2020/03/27	2020/03/23-03/30	12516	12392	626 ~ 1252
United Kingdom	2020/04/13	2020/04/05-04/14	86715	70811	4336 ~ 8672
Australia					
Australia	2020/03/28	2020/03/25-03/30	3482	3384	174 ~ 348

* Peak date has been observed. Due to the fluctuation of the daily reported cases, the observed peak interval was listed in stead of the exact peak date.

The number of maximum cases at the peak is the accumulated number of cases at the peak period.

The number of ventilator for the peak requirement is calculated based on the predicted infection. We assume 5 – 10% of the infected patients need the ventilator²².

Table 4: Estimated Medium R_t (95%CI) in the subsequent week

		First week	Second week	Third week	Fourth week	
Asia	China	1.64(0.98, 2.30)	1.34(1.21, 1.48)	0.59(0.55, 0.63)	0.26(0.24, 0.28)	
	Hubei Province, China	3.11(2.58, 3.64)	2.05(1.86, 2.23)	0.73(0.68, 0.77)	0.26(0.23, 0.29)	
	Wuhan, China	2.50(1.56, 3.44)	1.51(0.83, 2.19)	0.64(0.40, 0.88)	0.27(0.17, 0.37)	
	India	2.34(1.31, 3.38)	1.23(0.83, 1.63)	1.12(0.81, 1.42)	1.02(0.71, 1.32)	
	Indonesia	4.49(3.66, 5.31)	1.77(1.30, 2.23)	1.24(0.98, 1.51)	0.99(0.87, 1.11)	
	Iran	3.56(2.39, 4.73)	2.01(1.78, 2.23)	1.37(1.21, 1.53)	1.05(0.94, 1.16)	
	Israel	7.70(3.86, 11.55)	4.26(2.79, 5.73)	2.36(1.88, 2.83)	1.30(1.16, 1.45)	
	Japan	4.36(3.21, 5.50)	1.89(1.55, 2.22)	1.02(0.90, 1.14)	0.68(0.60, 0.76)	
	SKorea	1.52(0.99, 2.06)	1.42(0.99, 1.84)	1.32(0.98, 1.65)	1.22(0.96, 1.49)	
	Malaysia	5.77(4.81, 6.72)	3.39(2.77, 4.02)	2.19(1.66, 2.72)	1.46(1.18, 1.74)	
	Pakistan	4.90(3.58, 6.22)	2.32(1.82, 2.83)	1.02(0.86, 1.18)	0.71(0.60, 0.82)	
	Philippines	4.18(1.20, 7.17)	2.59(1.31, 3.87)	1.60(1.12, 2.09)	0.99(0.83, 1.16)	
	Saudi Arabia	2.91(1.55, 4.27)	2.14(1.53, 2.75)	1.57(1.33, 1.80)	1.15(0.97, 1.33)	
	Singapore	1.38(1.05, 1.72)	0.95(0.77, 1.14)	0.70(0.59, 0.81)	0.54(0.47, 0.61)	
	Thailand	6.03(4.55, 7.50)	2.99(2.60, 3.37)	1.48(1.38, 1.58)	0.73(0.63, 0.84)	
	Turkey	5.53(4.10, 6.95)	1.97(1.85, 2.10)	1.08(0.95, 1.21)	-	
	North America	US	3.03(2.53, 3.54)	3.69(3.13, 4.26)	3.24(2.68, 3.79)	2.19(1.91, 2.47)
		Canada	2.92(2.50, 3.34)	2.25(1.60, 2.91)	2.45(1.78, 3.13)	2.00(1.58, 2.41)
Dominican Republic		3.91(2.87, 4.94)	1.16(0.52, 1.80)	0.84(0.60, 1.08)	-	
Mexico		2.78(1.80, 3.76)	2.45(2.00, 2.90)	2.16(1.99, 2.32)	1.90(1.68, 2.11)	
South America	Chile	5.29(4.03, 6.54)	2.33(1.78, 2.89)	1.31(1.09, 1.53)	0.85(0.76, 0.95)	
	Brazil	6.91(4.55, 9.27)	4.36(3.30, 5.41)	1.84(1.56, 2.12)	1.54(1.38, 1.71)	
	Colombia	5.37(3.82, 6.92)	2.55(1.90, 3.19)	1.34(1.13, 1.55)	1.07(0.90, 1.24)	
	Panama	4.89(2.67, 7.11)	2.03(1.51, 2.55)	1.41(1.07, 1.76)	1.00(0.70, 1.30)	
Europe	Austria	4.91(3.63, 6.19)	3.91(2.80, 5.01)	2.75(2.14, 3.36)	1.38(1.17, 1.58)	
	Belgium	6.61(4.95, 8.28)	4.27(3.36, 5.19)	2.67(2.26, 3.08)	1.76(1.59, 1.92)	
	Czechia	4.07(2.81, 5.33)	2.33(2.07, 2.59)	1.47(1.28, 1.67)	0.93(0.76, 1.09)	
	Finland	7.76(5.23, 10.28)	2.50(1.23, 3.78)	1.38(0.80, 1.97)	1.10(0.72, 1.48)	
	France	4.29(3.39, 5.19)	1.80(1.06, 2.54)	1.26(0.83, 1.69)	0.95(0.71, 1.18)	
	Germany	5.52(4.16, 6.88)	3.48(2.83, 4.13)	2.19(1.91, 2.48)	1.38(1.27, 1.49)	
	Ireland	4.08(2.88, 5.27)	1.77(1.36, 2.18)	1.15(0.92, 1.38)	0.76(0.63, 0.90)	
	Italy	12.36(10.99, 13.74)	5.14(4.52, 5.76)	3.11(2.77, 3.46)	1.91(1.71, 2.10)	
	Luxembourg	4.05(2.48, 5.63)	1.71(1.47, 1.94)	0.82(0.70, 0.94)	0.40(0.33, 0.47)	
	Netherlands	4.39(3.01, 5.77)	2.54(2.38, 2.70)	1.68(1.57, 1.79)	1.13(1.04, 1.22)	
	Norway	3.89(3.09, 4.70)	2.43(2.09, 2.77)	1.38(1.09, 1.66)	0.75(0.62, 0.89)	
	Poland	3.45(2.85, 4.05)	2.46(2.15, 2.77)	1.75(1.61, 1.90)	1.25(1.17, 1.33)	
	Portugal	5.87(4.44, 7.30)	4.30(3.38, 5.22)	3.24(2.74, 3.74)	1.83(1.68, 1.99)	
	Romania	3.42(2.06, 4.78)	2.40(1.73, 3.08)	1.69(1.38, 1.99)	1.19(1.06, 1.31)	
	Russia	3.41(2.61, 4.22)	2.71(2.28, 3.14)	2.15(1.97, 2.33)	1.70(1.62, 1.79)	
	Spain	9.26(6.73, 11.79)	5.54(4.34, 6.73)	3.31(2.78, 3.84)	1.98(1.76, 2.20)	
	Sweden	2.39(1.64, 3.14)	2.07(1.56, 2.58)	1.79(1.47, 2.12)	1.55(1.35, 1.75)	
Switzerland	6.39(4.64, 8.15)	3.77(3.05, 4.49)	2.22(1.95, 2.50)	1.31(1.18, 1.44)		
United Kingdom	7.46(5.18, 9.74)	5.26(4.00, 6.52)	3.71(3.06, 4.36)	2.62(2.30, 2.93)		
Australia	Australia	3.72(3.41, 4.03)	2.48(2.16, 2.79)	2.16(1.90, 2.41)	1.43(1.30, 1.57)	

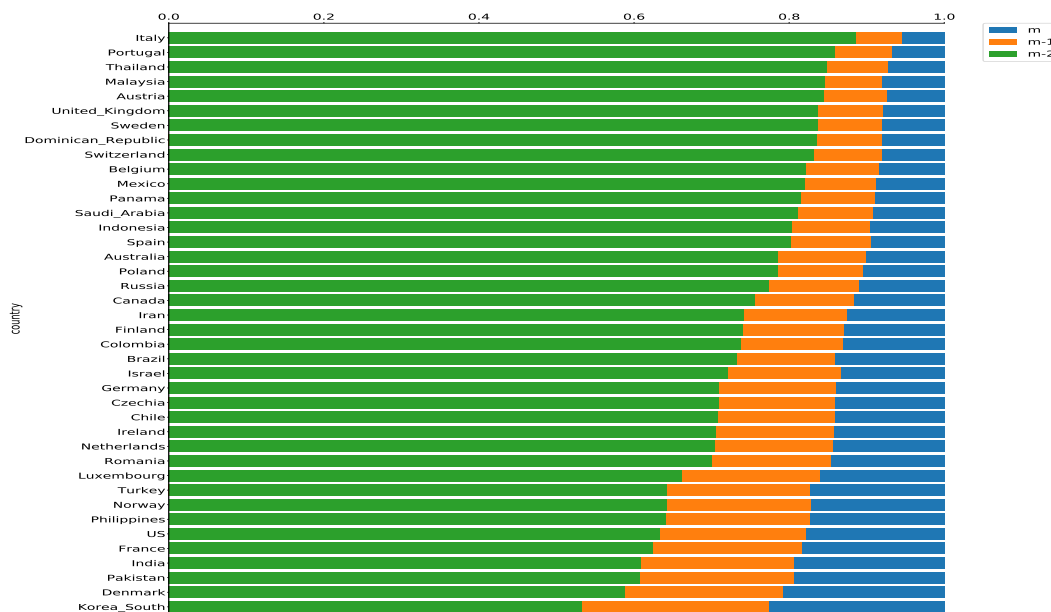


Figure 2: The proportion of epidemic size when the duration of infectious period m is reduced by 1 and 2. The reduction of infectious duration refers to shorten the time from the infection onset (symptomatic or asymptomatic) to isolation by intervention measures.

295 4. Discussions

296 Here we predicted that the COVID-19 pandemic will persistently spread
297 over many countries and will last on average 5 to 6 months since January 2020
298 for the current wave. We estimated, given no further intervention measures,
299 that India would emerge to be a new epidemic center, as well as Pakistan,
300 Brazil, Russia and Mexico. Effective intervention measures by reducing the
301 infectious period would result in an 50% reduction in the final epidemic sizes.
302 R_t had a declining trend in almost all countries, revealing the impact of the
303 intervention measures i.e. social distancing.

304 Our real-time estimation framework can yield a reliable prediction of
305 the final epidemic size using the data from the early phase of the epidemic.
306 We evaluated the performance of our model using incident case data from
307 January 20 to February 13, 2020 in China. We predicted the epidemic would
308 fade out on February 19 to 24 across 28 provinces in China with a one-
309 week lag in Wuhan; the epidemic size was estimated at 8,500 to 9,500, and
310 11,000 to 12,600 in 28 provinces and Hubei respectively. The outbreak size
311 and epidemic duration estimated are found to be highly consistent with the

312 observed figures (<https://www.who.int>). The prediction of the final epidemic
313 size based on the model that assumes early exponential growth could tend
314 to overestimate the epidemic size, which has been shown in the previous
315 studies^{10, 23-28}.

316 We estimated that the most affected countries in the next wave of the
317 pandemic will be India, Pakistan, Brazil, Mexico as well as Russia. All
318 these countries are currently undergoing regional or national lockdown except
319 Mexico. Given that thousands of ventilators are needed for the peak around
320 May to July, it is immediately important for these countries to prepare the
321 ICU beds. In Europe, most countries have peaked in the curve, and the final
322 outbreak size was estimated to exceed 10^5 in Italy, France, UK, Germany
323 and Spain. For the United States, the estimated final epidemic size will
324 surpass 1 million, peaking around July 2020. A recent report calculated that
325 81% of British and the United States populations would be infected, with
326 approximately a half and 2.2 million deaths respectively²⁹. The high value is
327 based on the assumption of R_0 at 2.4, while our results demonstrate that real-
328 time R_t decelerated under interventions. Thus, their estimates are likely to be
329 the higher bound of the true value. In Asia, besides China, South Korea and
330 Iran, Thailand and Malaysia have peaked in March. Indonesia and Saudi
331 Arabia would peak in April. Singapore and Japan recently implemented
332 lockdown and more data will be needed for the epidemic prediction. Given
333 the case-fatality rate at 2.3%⁶, we estimated around 23,000 deaths in India
334 and Pakistan, and around 2,300 in Mexico and Brazil, and 6,900 in Russia.

335 This is the first study to compare country-specific temporal R_t . It is
336 natural to expect a declining trend of R_t to 1 owing to stochastic effects for
337 epidemics governed by subexponential growth^{18, 30}, while a faster decline may
338 suggest a larger impact of intervention measures or behavior changes³¹. A
339 majority of countries displayed R_t below 5 in the first week of the epidemic
340 period. Several countries exhibited large R_t , ie. Italy or Spain, suggesting
341 a rapid increase of cases at the beginning or a large variation in the under-
342 reporting rates in the early epidemic phase. For Wuhan, R_t declined from
343 the median 2.5 to 0.3 within a month, which is compatible with the R_0 esti-
344 mation in a range of 2.2 to 3.6 in Wuhan^{2, 10, 12, 13, 16, 23, 31}, and below 1 after
345 interventions³². All countries displayed a declined trend towards 1 in the
346 epidemic period with varying deceleration rates, revealing the variation in
347 the impact of the intervention strategies. For further research on the in-
348 tervention effectiveness, individual data, as well as a series of intervention
349 measures for each country, may be required to quantify the effects in detail.

350 Our study showed that by shortening the infectious period by two days,
351 we could effectively reduce the final epidemic size by up to 50%. What
352 strategies can effectively reduce the infectious period? Usually, it can be
353 done - similar to the other coronaviruses - by early detection and isolation of
354 symptomatic patients and tracing of close contacts. However, the presymp-
355 tomatic transmission has been reported in many countries such as China,
356 the US, and Singapore³³⁻³⁶, etc. The existence of presymptomatic or asymp-
357 tomatic transmission would present difficult challenges for disease control,
358 which underscores the importance of social distancing. For instance, at the
359 onset of the epidemic, the spread has been well controlled in Singapore, ac-
360 counted for by a range of intervention measures, such as contact tracing and
361 quarantining, that were instituted from January 23-the onset of the first case
362 in Singapore³⁷. However, the recent increase in cases in Singapore, initially
363 starting from the imported cases followed by the outbreak in dormitories of
364 immigration workers, led to its circuit period from April 7 to May 4. Quar-
365 antine measures for the infected regions or at the national scale, either a
366 complete lockdown as in China or partial lockdown such as in Europe, are
367 effective in flattening the curve³⁸. Besides the quarantine measures, South
368 Korea was also successful in suppressing the outbreak, attributed to the
369 rapid measures to perform large-scale diagnostic testing for the public for
370 case isolation³⁹.

371 During the early phase of the epidemic, we forecasted the epidemic size
372 as a function of the time-varying growth model, similar but more flexible to
373 the previous approaches to model sub-exponential growth dynamics^{18-21, 40},
374 without relying on any epidemiological parameter assumptions. The tradi-
375 tional transmission epidemiological model is defined through a susceptible,
376 exposure, infectious, removed (SEIR) scheme, which requires epidemiological
377 parameters from detailed case studies^{2, 10, 31, 41}. Furthermore, given the varia-
378 tion of the transmissibility, mostly due to the intervention strategies imple-
379 mented and behavioral changes in the population, it is desirable to quantify
380 the dynamics of R_t over time^{20, 42-44}. Several studies attempted to forecast
381 the number of epidemics for COVID-19 in China using the constant growth
382 rate^{27, 45, 46}, which is not the case in our model of nonmonotonic behavior
383 of the growth rate. Our model, compared to previous studies, has greater
384 flexibility in a data-mining manner to fit and predict future trajectories.

385 In summary, we compared the epidemic trajectory, characterized dynamic
386 R_t in 42 countries, and predicted that the new epidemic centers will continue
387 to emerge in the next wave. Meanwhile, we highlighted the importance

388 of various effective interventions in flattening the epidemic curve, such as
389 social distancing, to shorten the infectious period. By carefully characterizing
390 the shape of the epidemic growth phase, we believe our study represents a
391 significant step in modeling real-time transmission and providing accurate
392 forecasts of epidemics.

393 Our study has several limitations. Firstly, the projection of the temporal
394 trend of an outbreak using the early-stage dataset could be dramatically
395 influenced by the changes in the intervention strategies later on. For example,
396 using data up to March 15, our previous analysis overestimated the epidemic
397 size in U.S as the social distance measures (i.e. quarantine) were implemented
398 starting from March 21. The performance of models used in this work will be
399 continuously improved with data coming in from an ongoing outbreak, thus
400 real-time estimates of key epidemiological parameters can be available before
401 the epidemic fully ends. Secondly, the number of infections estimated might
402 not be comparable across the countries; for example, the number of infections
403 in Germany is not comparable to the number of infections in Italy or China,
404 as the latter did not perform large-scale population-based testing and thus
405 the cases could be more severe. Lastly, the analyses are highly reliant on the
406 reporting criteria and quality of the data. The under-reporting of infection is
407 likely a common scenario in the majority of countries. For example, a recent
408 study showed that the reported number of confirmed positive cases was 50-
409 85-fold lower than the actual number of infections in 3330 people in Santa
410 Clara County, US⁴⁷. A more realistic and comprehensive analysis could be
411 performed that includes accurate epidemic data and information. In current
412 imperfect situation, our model could still be used for more advanced analyses,
413 including estimations of the epidemic size, peak points and dynamic R_t .

414 **Declaration of interests**

415 We declare no competing interests.

416 **Acknowledgments**

417 The research were partially supported by National Natural Science Foun-
418 dation of China (Nos. 11931014 and 11829101) and Fundamental Research
419 Funds for the Central Universities (No. JBK1806002) of China.

420 References

- 421 [1] D. Wang, B. Hu, C. Hu, F. Zhu, X. Liu, J. Zhang, B. Wang, H. Xiang,
422 Z. Cheng, Y. Xiong, et al., Clinical characteristics of 138 hospitalized pa-
423 tients with 2019 novel coronavirus–infected pneumonia in wuhan, china,
424 *Jama*.
- 425 [2] Q. Li, X. Guan, P. Wu, X. Wang, L. Zhou, Y. Tong, R. Ren, K. S.
426 Leung, E. H. Lau, J. Y. Wong, et al., Early transmission dynamics in
427 wuhan, china, of novel coronavirus–infected pneumonia, *New England*
428 *Journal of Medicine*.
- 429 [3] R. Lu, X. Zhao, J. Li, P. Niu, B. Yang, H. Wu, W. Wang, H. Song,
430 B. Huang, N. Zhu, et al., Genomic characterisation and epidemiology
431 of 2019 novel coronavirus: implications for virus origins and receptor
432 binding, *The Lancet*.
- 433 [4] P. Zhou, X.-L. Yang, X.-G. Wang, B. Hu, L. Zhang, W. Zhang, H.-R.
434 Si, Y. Zhu, B. Li, C.-L. Huang, et al., A pneumonia outbreak associated
435 with a new coronavirus of probable bat origin, *Nature* (2020) 1–4.
- 436 [5] D. K. Chu, Y. Pan, S. Cheng, K. P. Hui, P. Krishnan, Y. Liu, D. Y.
437 Ng, C. K. Wan, P. Yang, Q. Wang, et al., Molecular diagnosis of a
438 novel coronavirus (2019-ncov) causing an outbreak of pneumonia, *Clinical*
439 *Chemistry*.
- 440 [6] Z. Wu, J. M. McGoogan, Characteristics of and important lessons from
441 the coronavirus disease 2019 (covid-19) outbreak in china: summary of
442 a report of 72 314 cases from the chinese center for disease control and
443 prevention, *Jama*.
- 444 [7] K. Sun, J. Chen, C. Viboud, Early epidemiological analysis of the coron-
445 avirus disease 2019 outbreak based on crowdsourced data: a population-
446 level observational study, *The Lancet Digital Health*.
- 447 [8] C. Dye, N. Gay, Modeling the sars epidemic, *Science* 300 (5627) (2003)
448 1884–1885.
- 449 [9] M. Gilbert, G. Pullano, F. Pinotti, E. Valdano, C. Poletto, P.-Y. Boëlle,
450 E. D’Ortenzio, Y. Yazdanpanah, S. P. Eholie, M. Altmann, et al., Pre-
451 paredness and vulnerability of african countries against importations of
452 covid-19: a modelling study, *The Lancet*.

- 453 [10] J. T. Wu, K. Leung, G. M. Leung, Nowcasting and forecasting the poten-
454 tial domestic and international spread of the 2019-ncov outbreak origi-
455 nating in wuhan, china: a modelling study, *The Lancet*.
- 456 [11] S. Zhao, Q. Lin, J. Ran, S. S. Musa, G. Yang, W. Wang, Y. Lou, D. Gao,
457 L. Yang, D. He, et al., Preliminary estimation of the basic reproduction
458 number of novel coronavirus (2019-ncov) in china, from 2019 to 2020:
459 A data-driven analysis in the early phase of the outbreak, *International*
460 *Journal of Infectious Diseases*.
- 461 [12] Y. Liu, A. A. Gayle, A. Wilder-Smith, J. Rocklöv, The reproductive
462 number of covid-19 is higher compared to sars coronavirus, *Journal of*
463 *Travel Medicine*.
- 464 [13] J. Riou, C. L. Althaus, Pattern of early human-to-human transmission
465 of wuhan 2019 novel coronavirus (2019-ncov), december 2019 to january
466 2020, *Eurosurveillance* 25 (4).
- 467 [14] B. Efron, Bootstrap confidence intervals for a class of parametric prob-
468 lems, *Biometrika* 72 (1) (1985) 45–58.
- 469 [15] B. Efron, et al., Second thoughts on the bootstrap, *Statistical Science*
470 18 (2) (2003) 135–140.
- 471 [16] S. Zhao, Q. Lin, J. Ran, S. S. Musa, G. Yang, W. Wang, Y. Lou,
472 D. Gao, L. Yang, D. He, M. H. Wang, [Preliminary estimation of the](https://doi.org/10.1016/j.ijid.2020.01.050)
473 [basic reproduction number of novel coronavirus \(2019-ncov\) in china,](https://doi.org/10.1016/j.ijid.2020.01.050)
474 [from 2019 to 2020: A data-driven analysis in the early phase of the](https://doi.org/10.1016/j.ijid.2020.01.050)
475 [outbreak](https://doi.org/10.1016/j.ijid.2020.01.050), *International Journal of Infectious Diseases* 92 (2020) 214 –
476 217. doi:<https://doi.org/10.1016/j.ijid.2020.01.050>.
477 URL [http://www.sciencedirect.com/science/article/pii/](http://www.sciencedirect.com/science/article/pii/S1201971220300539)
478 [S1201971220300539](http://www.sciencedirect.com/science/article/pii/S1201971220300539)
- 479 [17] S. Zhao, S. S. Musa, H. Fu, D. He, J. Qin, Simple framework for real-
480 time forecast in a data-limited situation: the zika virus (zika) outbreaks
481 in brazil from 2015 to 2016 as an example, *Parasites & vectors* 12 (1)
482 (2019) 344.
- 483 [18] G. Chowell, L. Sattenspiel, S. Bansal, C. Viboud, Mathematical models
484 to characterize early epidemic growth: A review, *Physics of life reviews*
485 18 (2016) 66–97.

- 486 [19] C. Viboud, L. Simonsen, G. Chowell, A generalized-growth model to
487 characterize the early ascending phase of infectious disease outbreaks,
488 *Epidemics* 15 (2016) 27–37.
- 489 [20] S. Cauchemez, P.-Y. Boëlle, C. A. Donnelly, N. M. Ferguson,
490 G. Thomas, G. M. Leung, A. J. Hedley, R. M. Anderson, A.-J. Valleron,
491 Real-time estimates in early detection of sars, *Emerging infectious dis-
492 eases* 12 (1) (2006) 110.
- 493 [21] M. Lipsitch, T. Cohen, B. Cooper, J. M. Robins, S. Ma, L. James,
494 G. Gopalakrishna, S. K. Chew, C. C. Tan, M. H. Samore, other, Trans-
495 mission dynamics and control of severe acute respiratory syndrome, *Sci-
496 ence*.
- 497 [22] W.-j. Guan, Z.-y. Ni, Y. Hu, W.-h. Liang, C.-q. Ou, J.-x. He, L. Liu,
498 H. Shan, C.-l. Lei, D. S. Hui, et al., Clinical characteristics of coronavirus
499 disease 2019 in china, *New England Journal of Medicine*.
- 500 [23] H. Wang, Z. Wang, Y. Dong, R. Chang, C. Xu, X. Yu, S. Zhang,
501 L. Tsamlag, M. Shang, J. Huang, et al., Phase-adjusted estimation of
502 the number of coronavirus disease 2019 cases in wuhan, china, *Cell Dis-
503 covery* 6 (1) (2020) 1–8.
- 504 [24] M. Shen, Z. Peng, Y. Xiao, L. Zhang, Modelling the epidemic trend of
505 the 2019 novel coronavirus outbreak in china, *bioRxiv*.
- 506 [25] J. M. Read, J. R. Bridgen, D. A. Cummings, A. Ho, C. P. Jewell, Novel
507 coronavirus 2019-ncov: early estimation of epidemiological parameters
508 and epidemic predictions, *medRxiv*.
- 509 [26] M. A. Al-qaness, A. A. Ewees, H. Fan, M. Abd El Aziz, Optimization
510 method for forecasting confirmed cases of covid-19 in china, *Journal of
511 Clinical Medicine* 9 (3) (2020) 674.
- 512 [27] N. Imai, I. Dorigatti, A. Cori, C. Donnelly, S. Riley, N. M. Ferguson,
513 Report 2: Estimating the potential total number of novel coronavirus
514 cases in wuhan city, china, Imperial College London.
- 515 [28] S. Zhao, S. S. Musa, Q. Lin, J. Ran, G. Yang, W. Wang, Y. Lou,
516 L. Yang, D. Gao, D. He, et al., Estimating the unreported number of
517 novel coronavirus (2019-ncov) cases in china in the first half of january

- 518 2020: a data-driven modelling analysis of the early outbreak, *Journal of*
519 *clinical medicine* 9 (2) (2020) 388.
- 520 [29] N. Ferguson, D. Laydon, G. Nedjati Gilani, N. Imai, K. Ainslie,
521 M. Baguelin, S. Bhatia, A. Boonyasiri, Z. Cucunuba Perez, G. Cuomo-
522 Dannenburg, et al., Report 9: Impact of non-pharmaceutical interven-
523 tions (npis) to reduce covid19 mortality and healthcare demand.
- 524 [30] G. Chowell, C. Viboud, L. Simonsen, S. M. Moghadas, Characteriz-
525 ing the reproduction number of epidemics with early subexponential
526 growth dynamics, *Journal of The Royal Society Interface* 13 (123) (2016)
527 20160659.
- 528 [31] T. Liu, J. Hu, M. Kang, L. Lin, H. Zhong, J. Xiao, G. He, T. Song,
529 Q. Huang, Z. R. and, Transmission dynamics of 2019 novel coronavirus
530 (2019-ncov).
- 531 [32] A. J. Kucharski, T. W. Russell, C. Diamond, Y. Liu, J. Ed-
532 munds, S. Funk, R. M. Eggo, F. Sun, M. Jit, J. D. Munday,
533 N. Davies, A. Gimma, K. van Zandvoort, H. Gibbs, J. Hellewell,
534 C. I. Jarvis, S. Clifford, B. J. Quilty, N. I. Bosse, S. Abbott,
535 P. Klepac, S. Flasche, [Early dynamics of transmission and control](#)
536 [of covid-19: a mathematical modelling study](#), *The Lancet Infectious*
537 *Diseases* doi:[https://doi.org/10.1016/S1473-3099\(20\)30144-4](https://doi.org/10.1016/S1473-3099(20)30144-4).
538 URL [http://www.sciencedirect.com/science/article/pii/](http://www.sciencedirect.com/science/article/pii/S1473309920301444)
539 [S1473309920301444](http://www.sciencedirect.com/science/article/pii/S1473309920301444)
- 540 [33] G. Qian, N. Yang, A. H. Y. Ma, L. Wang, G. Li, X. Chen, X. Chen, A
541 covid-19 transmission within a family cluster by presymptomatic infec-
542 tors in china, *Clinical Infectious Diseases*.
- 543 [34] W. E. Wei, Presymptomatic transmission of sars-cov-2—singapore, jan-
544 uary 23–march 16, 2020, *MMWR. Morbidity and Mortality Weekly Re-*
545 *port* 69.
- 546 [35] L. Tian, X. Li, F. Qi, Q.-Y. Tang, V. Tang, J. Liu, X. Cheng, X. Li,
547 Y. Shi, H. Liu, et al., Pre-symptomatic transmission in the evolution of
548 the covid-19 pandemic, arXiv preprint arXiv:2003.07353.

- 549 [36] A. Kimball, Asymptomatic and presymptomatic sars-cov-2 infections in
550 residents of a long-term care skilled nursing facility—king county, wash-
551 ington, march 2020, MMWR. Morbidity and mortality weekly report
552 69.
- 553 [37] J. E. L. Wong, Y. S. Leo, C. C. Tan, [COVID-19 in Singapore—](#)
554 [Current Experience: Critical Global Issues That Require Attention](#)
555 [and Action](#), JAMAarXiv:[https://jamanetwork.com/journals/](https://jamanetwork.com/journals/jama/articlepdf/2761890/jama_wong_2020_vp_200026.pdf)
556 [jama/articlepdf/2761890/jama_wong_2020_vp_200026.pdf](https://jamanetwork.com/journals/jama/articlepdf/2761890/jama_wong_2020_vp_200026.pdf),
557 [doi:10.1001/jama.2020.2467](https://doi.org/10.1001/jama.2020.2467).
558 URL <https://doi.org/10.1001/jama.2020.2467>
- 559 [38] A. L. Phelan, R. Katz, L. O. Gostin, [The Novel Coronavirus Originating](#)
560 [in Wuhan, China: Challenges for Global Health Governance](#), JAMA
561 323 (8) (2020) 709–710. arXiv:[https://jamanetwork.com/journals/](https://jamanetwork.com/journals/jama/articlepdf/2760500/jama_phelan_2020_vp_200008.pdf)
562 [jama/articlepdf/2760500/jama_phelan_2020_vp_200008.pdf](https://jamanetwork.com/journals/jama/articlepdf/2760500/jama_phelan_2020_vp_200008.pdf),
563 [doi:10.1001/jama.2020.1097](https://doi.org/10.1001/jama.2020.1097).
564 URL <https://doi.org/10.1001/jama.2020.1097>
- 565 [39] R. M. Anderson, H. Heesterbeek, D. Klinkenberg, T. D. Hollingsworth,
566 How will country-based mitigation measures influence the course of the
567 covid-19 epidemic?, *The Lancet*.
- 568 [40] L. Forsberg White, M. Pagano, A likelihood-based method for real-time
569 estimation of the serial interval and reproductive number of an epidemic,
570 *Statistics in medicine* 27 (16) (2008) 2999–3016.
- 571 [41] X.-S. Zhang, R. Pebody, A. Charlett, D. de Angelis, P. Birrell, H. Kang,
572 M. Baguelin, Y. H. Choi, Estimating and modelling the transmissibility
573 of middle east respiratory syndrome coronavirus during the 2015 out-
574 break in the republic of korea, *Influenza and other respiratory viruses*
575 11 (5) (2017) 434–444.
- 576 [42] Q.-H. Liu, M. Ajelli, A. Aleta, S. Merler, Y. Moreno, A. Vespignani,
577 Measurability of the epidemic reproduction number in data-driven con-
578 tact networks, *Proceedings of the National Academy of Sciences* 115 (50)
579 (2018) 12680–12685.
- 580 [43] L. M. Bettencourt, R. M. Ribeiro, Real time bayesian estimation of the
581 epidemic potential of emerging infectious diseases, *PLoS One* 3 (5).

- 582 [44] A. N. Desai, M. U. Kraemer, S. Bhatia, A. Cori, P. Nouvellet, M. Her-
583 ringer, E. L. Cohn, M. Carrion, J. S. Brownstein, L. C. Madoff, et al.,
584 Real-time epidemic forecasting: Challenges and opportunities, *Health*
585 *security* 17 (4) (2019) 268–275.
- 586 [45] S.-m. Jung, A. R. Akhmetzhanov, K. Hayashi, N. M. Linton, Y. Yang,
587 B. Yuan, T. Kobayashi, R. Kinoshita, H. Nishiura, Real-time estimation
588 of the risk of death from novel coronavirus (covid-19) infection: Inference
589 using exported cases, *Journal of clinical medicine* 9 (2) (2020) 523.
- 590 [46] S. W. Hermanowicz, Forecasting the wuhan coronavirus (2019-ncov)
591 epidemics using a simple (simplistic) model, medRxiv.
- 592 [47] E. Bendavid, et al., Covid-19 antibody seroprevalence in santa clara
593 county, california, medRxiv, 2020.04.14.20062463 69.